# Relativistic Force Field: Parametrization of $^{13}C-^{1}H$ Nuclear Spin–Spin Coupling Constants

Andrei G. Kutateladze* and Olga A. Mukhina

Department of Chemistry and Biochemistry, University of Denver, Denver, Colorado 80208, United States

Ⓢ *Supporting Information*

ABSTRACT: Previously, we reported a reliable DU8 method for natural bond orbital (NBO)-aided parametric scaling of Fermi contacts to achieve fast and accurate prediction of proton–proton spin–spin coupling constants (SSCC) in ^{1}H NMR. As sophisticated NMR experiments for precise measurements of carbon–proton SSCCs are becoming more user-friendly and broadly utilized by the organic chemistry community to guide and inform the process of structure determination of complex organic compounds, we have now developed a fast and accurate method for computing $^{13}C-^{1}H$ SSCCs. Fermi contacts computed with the DU8 basis set are scaled using selected NBO parameters in conjunction with empirical scaling coefficients. The method is optimized for inexpensive B3LYP/6-31G(d) geometries. The parametric scaling is based on a carefully selected training set of 274 (^{3}J), 193 (^{2}J), and 143 (^{1}J) experimental $^{13}C-^{1}H$ spin–spin coupling constants reported in the literature. The DU8 basis set, optimized for computing Fermi contacts, which by design had evolved from optimization of a collection of inexpensive 3-21G*, 4-21G, and 6-31G(d) bases, offers very short computational (wall) times even for relatively large organic molecules containing 15–20 carbon atoms. The most informative SSCCs for structure determination, i.e., ^{3}J, were computed with an accuracy of 0.41 Hz (rmsd). The new unified approach for computing $^{1}H-^{1}H$ and $^{13}C-^{1}H$ SSCCs is termed "DU8c".
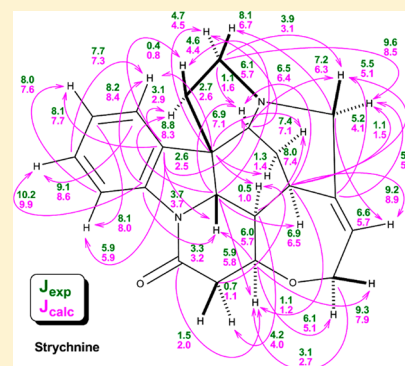
INTRODUCTION

Fast and accurate computations of spin–spin coupling constants (SSCC) for predicting NMR spectra have been challenging. Taking advantage of the fact that the Fermi contact (FC) mechanism dominates nuclear spin scalar couplings,[1] Bally and Rablen[2] have developed a basis set for a single parameter linear scaling of Fermi contacts, which can be used to obtain reasonably accurate estimates of proton–proton SSCCs. We refer the reader to their paper for an excellent overview of the field. Recently, we developed a multiparametric approach to scaling of Fermi contacts based on a representative set of SSCC "types" defined by connectivity and hybridization (for example, geminal sp^2 or vicinal sp^2-sp^3, etc.), i.e., not unlike the parametrization (force fields) in molecular mechanics.[3] We termed this approach "Relativistic Force Field". The first version of this approach, DU4, was further streamlined with simpler and more general parametric scaling scheme, which included NBO hybridization parameters. This was rationalized based on a paper by Weinhold, Markley, and coauthors[4] regarding the interpretation of scalar J-couplings in terms of natural bond orbitals (NBOs), which provided additional understanding of the nuances of applying Weinhold's NBO analysis[5] to the evaluation of Fermi contacts. As of now, the latest version of the method (and basis set), DU8,[6] consistently gives fast and accurate (0.2–0.4 Hz rmsd) predictions of proton–proton SSCCs for large organic molecules.

There is no such method for fast computations of $^{13}C-^{1}H$ SSCCs. The current state-of-the-art computations of

carbon–proton SSCCs require molecular structures optimized at very high levels of theory, computations of dia- and paramagnetic components of spin–orbit coupling, and hyperfine coupling with contributions from local, i.e., Fermi contacts (fc), and nonlocal spin-dipole interactions.[7] For example, Tormena and coauthors reported calculations of $^{3}J_{CH}$ values in a norbornane series of small organic molecules, resulting in adequate 0.3–0.4 Hz rmsd accuracy.[8] However, these DFT computations required geometry optimization with a aug-cc-pVTZ basis set[9] and calculations of all four terms for J_{CH}: (i) Fermi contact, (ii) spin dipolar, (iii) paramagnetic spin–orbit, and (iv) diamagnetic spin–orbit, which were carried out using Barone's EPR-III basis set.[10] Needless to say, these are very expensive computations, which took considerable CPU time even for such a small C_7 molecule as 2-norbornanone. As we will show below, for 2-norbornanone, our method delivers similar, if not slightly better, accuracy with a two order of magnitude reduction of computational time. This acceleration of computation is critical for larger molecules like strychnine ($C_{21}H_{22}N_2O_2$), for example, where the geometry optimization step with bases such as aug-cc-pVTZ is simply not a practical option.

RESULTS AND DISCUSSION

At this point, the issue of Fermi contacts dominating nuclear spin coupling constants is settled. It is also common knowledge

that calculations of spin−orbit and hyperfine coupling could be taxing and, in fact, could take orders of magnitude more computational time than calculations of Fermi contacts. As NBO dissection of spin−orbit coupling contributions is feasible,[11] we rationalized that all small perturbations on SSCCs can be approximated with an appropriate parametrization scheme, which includes NBO parameters, especially carbon's hybridization state. This approach proved fruitful for our prior DU8 parametrization of proton−proton constants.[6] Figure 1 shows schematic representation of natural hybrid
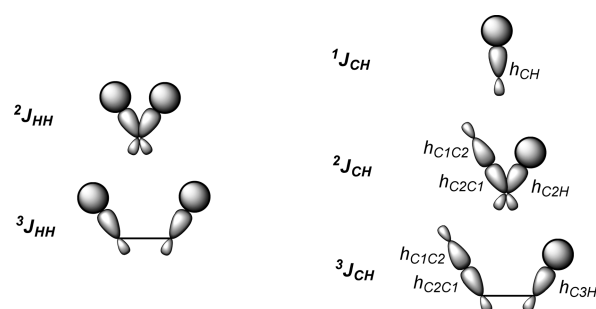

Figure 1. NHOs considered for ^2J-^3J geminal and vicinal pairs of protons (left) and ^1J-^3J carbons (right).

orbitals (NHOs) considered for geminal and vicinal proton−proton SSCCs (left) and carbon−proton SSCCs (right).

The training set was assembled with published experimental carbon−proton SSCCs found in several literature sources.[12] Specifically, we compiled a set of 274 ^3J, 193 ^2J, and 143 ^1J experimental ^{13}C−^{1}H spin−spin coupling constants.

Figure 2 gives the magnitude distributions for three sets of carbon−proton SSCCs: ^1J, ^2J, and ^3J. Expectedly, the majority of the one-bond (^1J) constants are in the range 140−200 Hz. The vicinal ^3J constants are well represented over the range of 2−10 Hz. The two bond (^2J) constants are smaller with the majority of them confined to the interval from −4 to +4 Hz.
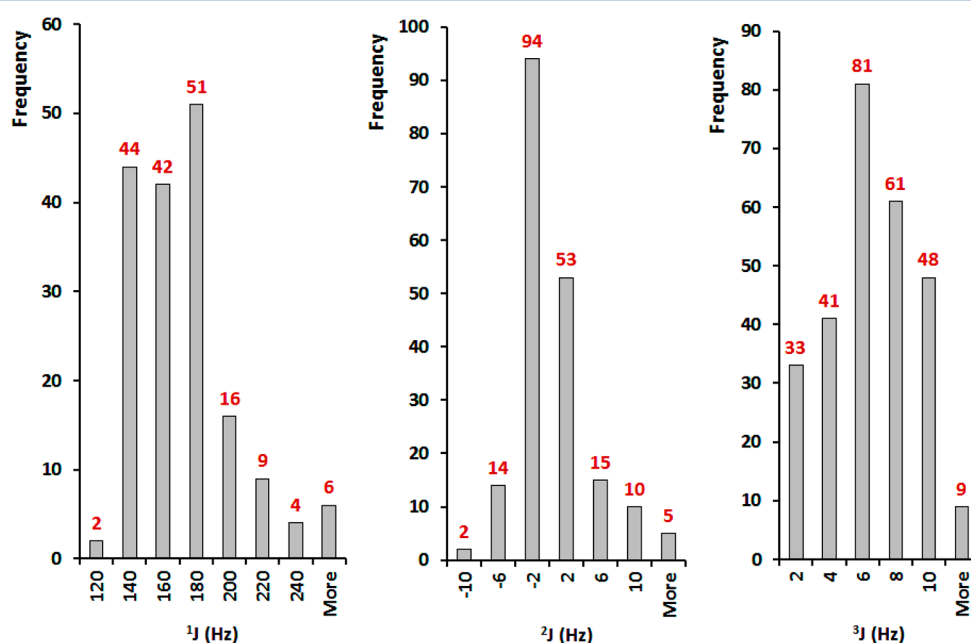
The parametric eqs (eqs 1−3), which were optimized with the DU8 basis set, had the following form

$$^3J_{CH} = c_9F^2 + (c_8H_{12} + c_7H_{13} + c_6H_{23})F + c_5H_{12} + c_4H_{13}$$
$$+ c_3H_{23} + c_2F + c_1 \qquad (1)$$

$$^2J_{CH} = c_9F^3 + (c_8H_{12} + c_7H_{13} + c_6H_{23})F + c_5H_{12} + c_4H_{13}$$
$$+ c_3H_{23} + c_2F + c_1 \qquad (2)$$

$$^1J_{CH} = c_9F^2 + c_6H_{23}F + c_3H_{23} + c_2F + c_1 \qquad (3)$$

where $H_{ij} = (1/(h_ih_j)^{1/2})$, with h_ih_j being the product of NBO hybridization coefficients,[13] weighing p-orbitals for the involved carbon atoms (see Supporting Information for details), F is the Fermi contact computed with the DU8 basis set for B3LYP/ 6-31G(d) geometry, and c_1−c_9 are empirical coefficients optimized via multivariate regression analysis. As with proton− proton SSCCs, in addition to the hybridization p-coefficients, h_C and h_X, we considered including the NBO second order perturbation energy, E(2), into the multivariate regression analysis as a variable for scaling of Fermi contacts. The second order perturbation energy was central to Weinhold's discussion of "how J-coupling, or rather the transfer of spin density, is related to spin hyperconjugative delocalization (by means of second order perturbation analysis)...".[4] As it was with proton SSCCs, we found little evidence for improvement of Fermi contact scaling with E(2) inclusion in C−H SSCC computations: the Student's t test values for the respective coefficient in the multivariate expression were very low (<1). Our rationale here is that Fermi contacts are dominated by these second order perturbative interactions, whereas we needed to identify the NBO elements that do not improve the computations of Fermi contacts but rather help correct for other (missing) contributors to SSCCs, such as dia- and paramagnetic components of spin−orbit coupling.

It is essential that in anticipation of the additional four terms in the parametric scaling equations for ^2J and ^3J that we compile
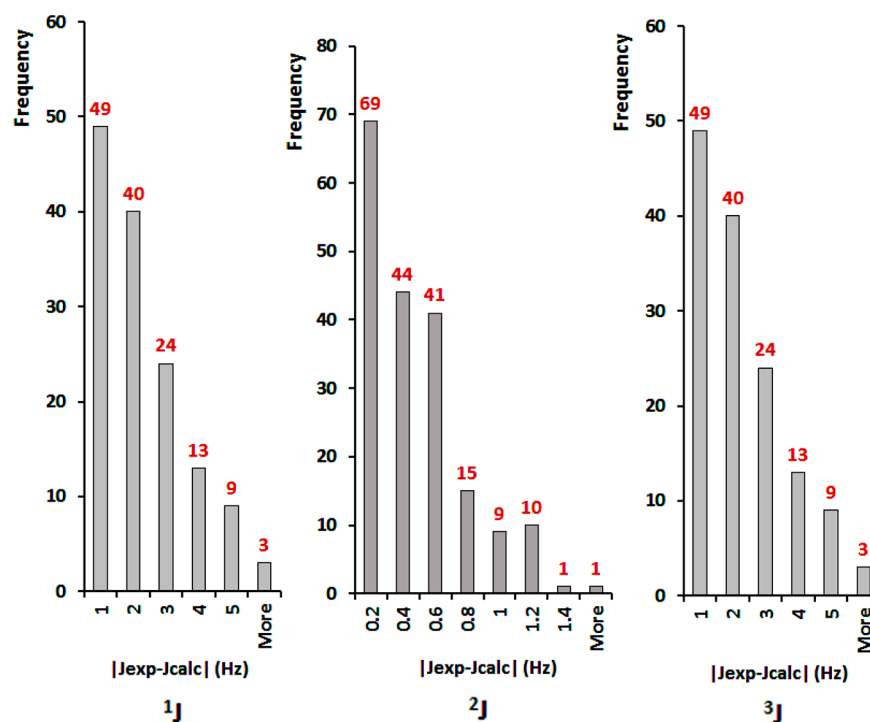

Figure 2. Magnitude distribution histograms for experimental ^1J, ^2J, and ^3J SSCCs in the training set.

10839

Figure 3. Unsigned error distribution histograms for calculated ^1J, ^2J, and ^3J SSCCs in the training set; rmsd: 2.28 Hz (^1J), 0.49 Hz (^2J), and 0.41 Hz (^3J).

Table 1. DU8c: Scaling Coefficients for J_{CH}

	c_9 $(F^n)^a$	c_8 (HF)	c_7 (HF)	c_6 (HF)	c_5 (H)	c_4 (H)	c_3 (H)	c_2 (F)	c_1 (const)	rmsd/N^b
$^1J_{CH}$	0.00017			−0.188			91.594	0.962	31.41	2.28/143
$^2J_{CH}$	−0.00052	−0.878	0.927	1.816	−8.823	2.115	17.524	0.129	−4.49	0.49/193
$^3J_{CH}$	0.00413	−2.345	2.772	−0.006	6.394	−5.983	−1.896	0.752	0.68	0.41/274
other								0.71		

^{a}n = 2, except for geminal SSCCs, which required a cubic term to describe ^2J in C≡C−H. ^{b}N = number of experimental constants in the training set.

a sufficient number of experimental values in the test set: more than 20 experimental points per one optimized parametric coefficient c_i in the case of ^2J and more than 30 experimental points per one parametric coefficient in the case of ^3J. As ^3J values are particularly useful for structure elucidation, the training set of the experimental three-bond constants was the largest. The results of the multivariate fitting are summarized in Figure 3, which shows unsigned error distribution histograms for each SSCC type. The absolute rmsd values are highest for the large ^1J constants, but the *relative* error is the lowest in this case: only 1.4% for the average value of 161 Hz.

We determined that to adequately describe ^2J in C≡C−H moieties, for example, we needed a cubic term c_9 (eq 2 and Table 1). We then allowed for nonlinear terms in our fitting procedure and found a modest improvement with quadratic terms for ^1J and ^3J. There is an insufficient number of large experimental long-range ^{13}C−^1H constants, so for safety we chose to scale their Fermi contacts by a single factor of 0.71. All optimized scaling coefficients are listed in Table 1.

We then revisited our NBO-aided scaling of proton−proton SSCCs[6] and revised it to keep both ^1H−^1H and ^{13}C−^1H parametric schemes uniform. This revision did not produce any significant improvement, nor did it degrade the performance of the original DU8 prediction of ^1H−^1H SSCCs. To differentiate between the two, we will refer to the *unified* parametric

method, which now includes ^{13}C−^1H constants, as DU8c. The parametric equation for H−H constants is given in eq 4, and the scaling coefficients are summarized in Table 2.

$$^nJ_{HH} = c_9F^2 + c_6H_{23}F + c_3H_{23} + c_2F + c_1 \quad (4)$$

Table 2. DU8c: Scaling Coefficients for J_{HH}

	c_9 (F^2)	c_6 (HF)	c_3 (H)	c_2 (F)	c_1 (const)	rmsd/N^b
$^2J_{HH}$	0.00061	0.838	6.683	1.211	−3.38	0.24/151
$^3J_{HH}$	a	0.220	−1.036	1.431	0.41	0.17/471
$^4J_{HH}$	0.00021	0.272	0.541	1.344	a	0.12/187
$^5J_{HH}$	a	−0.620	0.447	1.346	a	0.10/29
other				0.71		

^{a}Coefficient is excluded from optimization due to low Student's t test value. ^{b}N = number of experimental constants in the training set.

As stated above, we termed this general approach Relativistic Force Field (RFF). The hybridization-derived empirical corrections to Fermi constants are parametrized for different bonding arrangements, not unlike force fields in molecular mechanics. The goal is to significantly accelerate computations of SSCCs with the minimal number of empirical parameters (24 for carbon−proton and 17 for proton−proton SSCCs).

Table 3. Comparison of $^3J_{CH}$ in Norbornanes Computed for Bridgehead Carbons and Protons by Tormena[8] and DU8c in this Work

	C(1)−H(4)					C(4)−H(1)				
	exp	ref 8	(Δ)	DU8c	(Δ)	exp	ref 8	(Δ)	DU8c	(Δ)
2-norbornanone	5.2	4.9	(0.3)	4.8	(0.4)	8.5	9.3	(−0.8)	8.8	(−0.3)
exo-3-chloro-2-norbornanone	5.3	5.0	(0.3)	5.0	(0.3)	8.4	8.6	(−0.2)	8.3	(0.1)
endo-3-chloro-2-norbornanone	5.0	4.9	(0.1)	4.9	(0.1)	8.0	8.4	(−0.4)	8.0	(0.0)
exo-3-bromo-2-norbornanone	5.3	5.0	(0.3)	5.0	(0.3)	8.6	8.8	(−0.2)	8.5	(0.1)
endo-3-bromo-2-norbornanone	4.9	4.8	(0.1)	4.9	(0.0)	8.1	8.4	(−0.3)	8.0	(0.1)
exo-norborneol	8.4	8.3	(0.1)	7.9	(0.5)	9.5	9.7	(−0.2)	8.8	(0.7)
endo-norborneol	7.7	7.2	(0.5)	7.3	(0.4)	8.8	9.3	(−0.5)	8.5	(0.3)

As we demonstrate below, this approach shows excellent accuracy while dramatically reducing the computational time.

Test Cases. Computational methods for evaluation of nuclear spin−spin coupling constants are available, but they are very expensive because small contributions of spin−orbit coupling and other terms require high quality geometries, very high quality wave functions, and take a long time to compute. An instructive example is a paper by Tormena and coauthors[8] investigating carbon−proton C(1)−H(4) and C(4)−H(1) spin−spin coupling constants in substituted norbornanes. For geometry optimization, they chose the aug-cc-pVTZ basis set followed by calculations of SSCCs evaluating all four terms (Fermi contact, spin dipolar, paramagnetic spin−orbit, and diamagnetic spin−orbit) as stipulated by Gaussian spinspin keyword using Barone's EPR-III basis set. They report "excellent agreement" with experimental values, achieving rmsd of 0.36 Hz on the total of 14 experimental SSCCs (Table 3).

On the same set of 14 SSCCs, DU8c delivered a comparable if not slightly better accuracy of 0.32 Hz. However, the most striking metric is the computational time on a 16-core node of a Linux cluster. This performance comparison for the smallest test system, 2-norbornanone, is presented in Table 4. Geometry

Table 4. Comparison of the Time Performance of DU8c and Full GIAO[8] for 2-Norbornanone

	ref 8	DU8c (this work)
CPU time for geometry optimization[a]	26.9 h	14.3 min
CPU time for SSCC calculations[a]	16.9 h	14.0 min
total time on a 16-core node	2.7 h	<2 min
accuracy (RMSD over 14 SSCCs)	0.36 Hz	0.32 Hz

[a]Calculations from ref 8 were reproduced on the same node for fair comparison.

optimization and calculations of SSCCs took a full 2 orders of magnitude less CPU time for DU8c. This time differential manifested itself for a rather small $C_7H_{10}O$ molecule. For molecular systems of larger size, DFT geometry optimizations using aug-cc-pVTZ basis set are prohibitively expensive. For example, our attempt to refine the geometry of strychnine at the B3LYP/aug-cc-pVTZ level produced a few SCF cycles over several days and did not converge. Another attempt to run our DFT SSCCs calculations for the B3LYP/6-311+G(d,p) geometry of strychnine with the EPR-III basis in conjunction with the Gaussian 09 spinspin keyword took more than a week and resulted in similar accuracy of 0.7 Hz. This compares unfavorably with our DU8c computations, which took approximately 6 min of wall time for geometry optimization and 17 min for calculations of H−H and C−H SSCCs for each of two conformers of strychnine. These short computational

times for a rather large ($C_{21}H_{22}N_2O_2$) molecule impart confidence that, in cases requiring conformational averaging over an ensemble of conformers, the method could be applied with the reasonable expectation of achieving a practical outcome within a sensible period time.

Strychnine has long been a favorite model compound for the NMR community, so we compiled the available literature data on its carbon−proton SSCCs to evaluate the accuracy of our computational predictions. Recent experimental work by Williamson, Buevich, Martin, and Parella[14] has arguably produced the most comprehensive set of carbon−proton spin−spin coupling constants for strychnine. For comparison, we augmented their data with nine additional data sets found in the literature (see Table 5; Figure 4 shows the strychnine numbering scheme).

The accuracy, i.e., rmsd, for *N* reported experimental values for each of the experimental data sets is shown at the bottom of Table 5. In addition to fast DU8c computations, we also reproduced the GIAO calculations of strychnine's $^{13}C-^1H$ SSCCs exactly as ran by the authors of ref 14 at the B3LYP/6-311++G(d,p)//B3LYP/6-311++G(d,p) level of theory. The accuracy of these GIAO computations was also compared for all ten experimental data sets in Table 5. It is clear from the comparison of DU8c and GIAO@B3LYP/6-311++G(d,p)//B3LYP/6-311++G(d,p) (see rmsds at the bottom of the table) that both calculations resulted in similar accuracy with DU8c performing marginally better. However, the CPU time differential was conspicuous (see Table 6). DU8c computations took 23 min of total (wall) time on a 16-core node, whereas computations of all (difficult) contributions to Js at the GIAO, B3LYP/6-311++G(d,p)//B3LYP/6-311++G(d,p) level of theory required almost 17 h.

Table 5 also highlights the existing challenges in obtaining accurate carbon−proton experimental constants: for example, $^3J_{C20-H22}$ is reported by seven sources with values ranging from 4.9 to 12.5 Hz and standard deviation approaching 3 Hz. It appears that the paper by Williamson and coauthors[14] contains the most extensive and reliable set of experimental constants for strychnine, yet the accuracy of some constants may still be questionable. For example, the two-bond constant $^2J_{C23-H22}$ is measured at 8.73 Hz, whereas the other five experimental values for this constant reported in the literature average to 6.54 Hz (with a small standard deviation of 0.6 Hz), which matches our calculated value of 6.49 Hz very well.

We also looked at a set of selected experimental constants matching the calculated best. It is curious that the accuracy on a cherry-picked set of constants approaches 0.43 Hz. The most stereochemically informative three-bond $^3J_{CH}$ SSCCs (total of 61) in this case are computed with an accuracy of 0.37 Hz. Although such artificial matching of the best fitted experimental

Table 5. DU8c-Calculated and Experimental[a] $^{n}J_{CH}$ in Strychnine (Excluding $^{1}J_{CH}$)

C	H	type	J_{calc}	exp (ref 14)	exp (ref 15a)	exp (ref 15c)	exp (ref 15b)	exp (ref 16)	exp (ref 17)	exp (ref 18)	exp (ref 19)	exp (ref 20a)	exp (ref 20b)
C1	H2	^2J	1.87	2.61 (0.7)						0.8 (1.1)			
C1	H3	^3J	8.56	9.1 (0.5)						8.5 (0.1)		8.9 (0.3)	9.3 (0.7)
C1	H4	^4J	−1.38	−1.34 (0)						−1.2 (0.2)			
C2	H1	^2J	0.50							0.9 (0.4)			
C2	H3	^2J	1.59	2.34 (0.7)						1.9 (0.3)			
C2	H4	^3J	7.96	8.07 (0.1)	7.5 (0.5)	7.4 (0.6)				7.4 (0.6)			
C3	H1	^3J	7.30	7.7 (0.4)						7.4 (0.1)			
C3	H2	^2J	1.78	2.43 (0.7)						2.6 (0.8)			
C3	H4	^2J	1.17	1.87 (0.7)						0.6 (0.6)			
C4	H1	^4J	−1.35	−1.36 (0)						−1 (0.3)			
C4	H2	^3J	7.64	7.96 (0.3)						7.9 (0.3)			
C4	H3	^2J	2.34	3.19 (0.9)						2.3 (0)		2.3 (0)	2.5 (0.2)
C5	H1	^3J	8.37	8.24 (0.1)									
C5	H11a	^4J	0.84	1.21 (0.4)									
C5	H11b	^4J	−0.62	−0.71 (0.1)									
C5	H2	^4J	−1.52	−1.56 (0)									
C5	H3	^3J	9.89	10.19 (0.3)									
C5	H4	^2J	−2.25	−2.04 (0.2)									
C5	H8	^3J	3.17	3.25 (0.1)	3.2 (0)	3.1 (0.1)					3.5 (0.3)	3.4 (0.2)	
C6	H1	^2J	0.64	1.2 (0.6)									
C6	H16	^3J	2.52	2.56 (0)									
C6	H17a	^3J	2.92	3.09 (0.2)									
C6	H17b	^3J	0.77	0.37 (0.4)									
C6	H2	^3J	7.72	8.08 (0.4)									
C6	H20b	^5J	0.35	0.44 (0.1)									
C6	H3	^4J	−1.46	−1.5 (0)									
C6	H4	^3J	5.94	5.85 (0.1)	5.5 (0.4)	5.5 (0.4)							
C6	H8	^3J	3.71	3.66 (0)	3.7 (0)	3.7 (0)					4 (0.3)	3.9 (0.2)	
C7	H1	^3J	2.55	2.66 (0.1)									
C7	H12	^4J	1.00	1.38 (0.4)									
C7	H13	^3J	0.98	0.5 (0.5)							1.9 (0.9)		
C7	H15a	^3J	7.11	7.42 (0.3)	7.2 (0.1)	7.3 (0.2)		7.3 (0.2)					
C7	H15b	^3J	1.42	1.34 (0.1)									
C7	H16	^2J	−1.21	−0.33 (0.9)									
C7	H17a	^2J	−3.15	−2.44 (0.7)									
C7	H17b	^2J	−3.42	−2.6 (0.8)									
C7	H18a	^3J	4.47	4.7 (0.2)	4.6 (0.1)	5.2 (0.7)		5.2 (0.7)				4.5 (0)	

Table 5. continued

C	H	type	J_{calc}	exp (ref 14)	exp (ref 15a)	exp (ref 15c)	exp (ref 15b)	exp (ref 16)	exp (ref 17)	exp (ref 18)	exp (ref 19)	exp (ref 20a)	exp (ref 20b)
C7	H2	^4J	0.56	0.82 (0.3)									
C7	H3	^5J	0.34	0.37 (0)									
C7	H4	^4J	0.34	0.47 (0.1)									
C7	H8	^2J	−2.49	−1.89 (0.6)	−2.5 (0)	−2.4 (0.1)		−2.6 (0.1)			−2.9 (0.4)		
C7	H11a	^4J	0.27	0.5 (0.2)									
C8	H12	^3J	5.82	5.94 (0.1)	5.8 (0)	5.9 (0.1)	5.8			5.7 (0.1)			
C8	H13	^2J	−5.51	−5.72 (0.2)	−6.3 (0.8)	−6.4 (0.9)	−6.3 (0.8)			−6.3 (0.8)	−6.2 (0.7)		
C8	H14	^3J	6.48	6.86 (0.4)						8.5 (2)			
C8	H16	^3J	7.09	6.87 (0.2)									
C8	H17a	^3J	8.60	8.83 (0.2)									
C8	H17b	^3J	4.33	4.61 (0.3)									
C10	H11a	^2J	−5.11	−5.66 (0.5)	−5.8 (0.7)	−6.5 (1.4)	−5.6 (0.5)	−6.4 (1.3)				−6.7 (1.6)	
C10	H11b	^2J	−7.43	−7.42 (0)	−7.9 (0.5)	−7.9 (0.5)		−7.4 (0)			−7.9 (0.5)	−7.7 (0.3)	
C10	H12	^3J	1.95	1.54 (0.4)			5.8 (3.8)				2 (0)		
C11	H12	^2J	−2.12	−1.05 (1.1)						−2.1 (0)		−2.2 (0.1)	−1.9 (0.2)
C11	H13	^3J	1.08	0.67 (0.4)						0.6 (0.5)		0.4 (0.7)	−0.5 (1.6)
C12	H11a	^2J	−2.08	−0.61 (1.5)	−2.5 (0.4)	−0.8 (1.3)	−0.8 (1.3)		−1.7 (0.4)	−2 (0.1)		−1.9 (0.2)	−2.1 (0)
C12	H11b	^2J	−6.12	−6.74 (0.6)	−7 (0.9)	−6.9 (0.8)		−7.1 (1)		−6.9 (0.8)		−6.9 (0.8)	−6.9 (0.8)
C12	H13	^2J	−1.77		−0.6 (1.2)	−0.8 (1)		−1.2 (0.6)	−1.2 (0.6)	−0.3 (1.5)	−1.7 (0.1)		
C12	H14	^3J	2.03							2 (0)			
C12	H23a	^3J	5.10	6.1 (1)	5.6 (0.5)	5.7 (0.6)						5.2 (0.1)	
C12	H23b	^3J	7.91	9.32 (1.4)	8.6 (0.7)	8.2 (0.3)						8.3 (0.4)	
C12	H8	^3J	5.66	6.03 (0.4)	5.5 (0.2)	5.6 (0.1)			5.4 (0.3)	5.5 (0.2)	5.7 (0)	5.8 (0.1)	5.6 (0.1)
C13	H11a	^3J	4.00	4.15 (0.2)	3.4 (0.6)	3.3 (0.7)							
C13	H11b	^3J	0.73	0.07 (0.7)						2.7 (2)			
C13	H12	^2J	0.24	1.63 (1.4)						1.7 (1.5)			
C13	H14	^2J	−5.01							−5.7 (0.7)			
C13	H15a	^3J	7.40	8.01 (0.6)	8 (0.6)	8.1 (0.7)		7.9 (0.5)	7.7 (0.3)				
C13	H15b	^3J	3.40		3.3 (0.1)	3.5 (0.1)		4.6 (1.2)	3.8 (0.4)				
C13	H17a	^4J	0.55	0.75 (0.2)									
C13	H20a	^4J	−0.88	−1.18 (0.3)									
C13	H22	^4J	−0.97	−1.38 (0.4)									
C13	H23a	^4J	1.49	2.15 (0.7)									
C13	H8	^2J	−1.89	−1.07 (0.8)						−1.6 (0.3)			
C14	H23a	^4J	−0.72							−0.3 (0.4)			
C14	H12	^3J	1.17	1.06 (0.1)									
C14	H13	^2J	−4.43	−4.04 (0.4)	−4.6 (0.2)	−4.7 (0.3)		−4.7 (0.3)		−5.4 (1)	−5.1 (0.7)	−5.5 (1.1)	−4.5 (0.1)

Table 5. continued

C	H	type	J_{calc}	exp (ref 14)	exp (ref 15a)	exp (ref 15c)	exp (ref 15b)	exp (ref 16)	exp (ref 17)	exp (ref 18)	exp (ref 19)	exp (ref 20a)	exp (ref 20b)
C14	H15a	^2J	−2.85	−1.8 (1.1)	−1.8 (1.1)	−2.8 (0.1)	−2.8 (0.1)	−3.2 (0.3)		−2.7 (0.2)		−1.2 (1.7)	−2.9 (0)
C14	H15b	^2J	−3.21	−2.29 (0.9)	−3.2 (0)	−3.6 (0.4)		−4.8 (1.6)		−3.3 (0.1)		−2.3 (0.9)	−2.6 (0.6)
C14	H16	^3J	6.35	6.5 (0.2)						6.4 (0.1)		6.7 (0.4)	6.4 (0.1)
C14	H20a	^3J	1.50	1.13 (0.4)									
C14	H20b	^3J	5.09	5.47 (0.4)	5.4 (0.3)	5.3 (0.2)		5.5 (0.4)		5.4 (0.3)			
C14	H22	^3J	8.92	9.16 (0.2)	7.9 (1)	8.5 (0.4)	8.6 (0.3)	8.9 (0)		6.6 (2.3)		8.5 (0.4)	8.6 (0.3)
C14	H8	^3J	0.52	0.2 (0.3)						0.3 (0.2)	−0.5 (1)		
C15	H13	^3J	3.27	3.71 (0.4)	3.5 (0.2)	3.4 (0.1)		6.6 (3.3)		6.3 (3)	4 (0.7)		
C15	H16	^2J	−2.12	−1.1 (1)						−2.2 (0.1)			
C15	H17b	^4J	0.59	0.9 (0.3)									
C15	H20a	^4J	0.46	0.84 (0.4)									
C15	H20b	^4J	0.86	1.44 (0.6)									
C15	H22	^4J	0.72	1.04 (0.3)									
C16	H14	^3J	6.04							7.2 (1.2)			
C16	H15a	^2J	−4.16	−3.6 (0.6)	−4.5 (0.3)	−4.3 (0.1)				−4.6 (0.4)			
C16	H15b	^2J	−2.56	−1.25 (1.3)	−2.7 (0.1)	−3 (0.4)				−2.8 (0.2)			
C16	H18a	^3J	5.67	6.13 (0.5)		4.3 (1.4)							
C16	H20b	^3J	6.34	7.16 (0.8)	6.9 (0.6)	6.9 (0.6)							
C16	H8	^3J	1.16	0.87 (0.3)							3.3 (2.1)		
C17	H1	^4J	−0.48	−0.65 (0.2)									
C17	H18a	^2J	−2.09	−0.79 (1.3)	−2.7 (0.6)	−3.2 (1.1)	−3.5 (1.4)	−2.4 (0.3)		−4.7 (2.6)			
C17	H18b	^2J	−3.98	−3.91 (0.1)	−5.6 (1.6)	−5.1 (1.1)		−4.9 (0.9)		−5 (1)			
C17	H20a	^4J	0.71	0.93 (0.2)									
C17	H3	^6J	−0.40	−0.6 (0.2)									
C17	H8	^3J	6.03	6.57 (0.5)	5.9 (0.1)	5.9 (0.1)		5.9 (0.1)			5.9 (0.1)		
C18	H16	^3J	1.64	1.14 (0.5)									
C18	H17a	^2J	−4.09	−3.77 (0.3)						−3.1 (1)			
C18	H17b	^2J	−0.56	−1.44 (0.9)						−3.1 (2.5)			
C18	H20a	^3J	8.48	9.64 (1.2)	9.3 (0.8)	9.6 (1.1)	9.5 (1)	9.5 (1)				9.3 (0.8)	
C18	H20b	^3J	3.13	3.87 (0.7)	3.5 (0.4)	3.1 (0)	3.4 (0.3)	3.6 (0.5)					
C20	H14	^3J	1.95							1.2 (0.8)			
C20	H15b	^4J	0.52	0.37 (0.1)									
C20	H18a	^3J	1.20	0.54 (0.7)									
C20	H18b	^3J	6.72	8.05 (1.3)	7.1 (0.4)	7.1 (0.4)	5.1 (0.6)	7.4 (0.7)		7.4 (1.7)		7.4 (0.7)	
C20	H22	^3J	5.74	6.6 (0.9)	4.9 (0.8)	5.6 (0.1)		12.5 (6.8)	5.7 (0)	−1 (0)			
C20	H23a	^4J	−0.99	−1.29 (0.3)									
C20	H23b	^4J	0.34	0.56 (0.2)						0.4 (0.1)			

Table 5. continued

C	H	type	J_{calc}	exp (ref 14)	exp (ref 15a)	exp (ref 15c)	exp (ref 15b)	exp (ref 16)	exp (ref 17)	exp (ref 18)	exp (ref 19)	exp (ref 20a)	exp (ref 20b)
C21	H13	^3J	6.91	7.77 (0.9)	7.8 (0.9)	7.5 (0.6)			7.4 (0.5)		7.55 (0.6)	7.5 (0.6)	7.5 (0.6)
C21	H14	^2J	−6.85								−5.8 (1)		
C21	H15a	^3J	1.23	1 (0.2)	0.9 (0.3)	1.4 (0.2)		1.9 (0.7)			1.3 (0.1)		
C21	H15b	^3J	6.32	6.54 (0.2)	6 (0.3)	6 (0.3)		6.1 (0.2)			6.5 (0.2)		
C21	H16	^4J	−0.51	−0.76 (0.2)							−1 (0.5)		
C21	H18b	^4J	0.42	0.54 (0.1)									
C21	H20a	^2J	−4.93	−3.34 (1.6)	−4.9 (0)	−4.6 (0.3)							
C21	H20b	^2J	−2.81	−1.68 (1.1)	−2.4 (0.4)	−1 (1.8)	−1 (1.8)						
C21	H23a	^3J	4.60	4.29 (0.3)	3.3 (1.3)	3.2 (1.4)							
C21	H23b	^3J	6.23	8.66 (2.4)	8.5 (2.3)	8.3 (2.1)							
C22	H14	^3J	4.88								5.7 (0.8)	8.3 (3.4)	
C22	H15a	^4J	−0.29	−0.41 (0.1)							−1.3 (1)		
C22	H15b	^4J	0.43	0.69 (0.3)							−0.7 (1.1)		
C22	H16	^5J	0.54	0.53 (0)							1.3 (0.8)		
C22	H20a	^3J	5.48	5.61 (0.1)	6.1 (0.6)	5.8 (0.3)						5.1 (0.4)	
C22	H20b	^3J	4.07	5.19 (1.1)	4.5 (0.4)	4.6 (0.5)						4.7 (0.6)	
C22	H23a	^2J	−4.50	−2.43 (2.1)	−3.8 (0.7)	−4 (0.5)				−3.8 (0.7)		−4.2 (0.3)	−3.8 (0.7)
C22	H23b	^2J	−3.58	−2.96 (0.6)	−4 (0.4)	−3.9 (0.3)				−3.7 (0.1)		−3.6 (0)	−3.4 (0.2)
C23	H12	^3J	2.66	3.07 (0.4)	2.4 (0.3)	6.8 (4.1)	2.4 (0.3)						
C23	H14	^4J	−0.97							−1.8 (0.8)			
C23	H20a	^4J	−0.87	−1.21 (0.3)									
C23	H22	^2J	6.49	8.73 (2.2)	5.7 (0.8)	7.1 (0.6)	7.1 (0.6)	6.2 (0.3)	7	6.6 (0.1)			
number of exp SSCCs				122	50	51	14	25	7	51	23	27	14
rmsd for DU8c (Hz)				0.7	0.7	0.9	1.3	1.7	0.4	1.0	0.8	0.9	0.6
rmsd for GIAO[b] (Hz)				0.6	0.9	1.0	1.6	1.7	0.6	1.3	1.1	1.2	0.9

[a]Δ|exp − calcd| is in parenthesis. [b]Full GIAO calculations at B3LYP/6-311++G(d,p)//B3LYP/6-311++G(d,p).
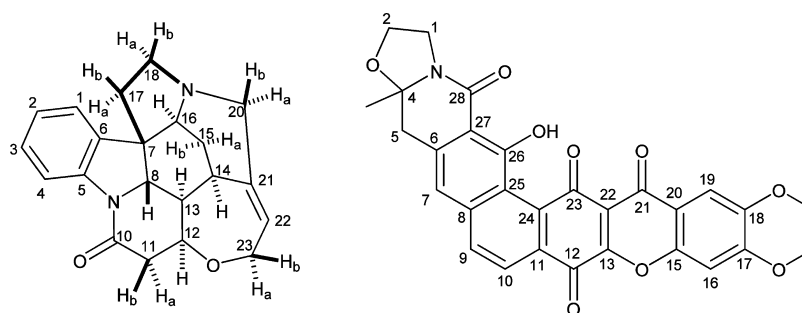
Figure 4. Numbering for strychnine (left) and cervinomycin A$_2$ (right).

Table 6. Time Performance Comparison of DU8c with the Full GIAO Calculations for Strychnine

	GIAO[a]	DU8c (this work)
CPU time for geometry optimization	18.4 h	1.5 h
CPU time for SSCC calculations	247.4 h	4.4 h

[a]GIAO, B3LYP/6-311++G(d,p)//B3LYP/6-311++G(d,p).

values is not an advisable way of assessing the accuracy of any computational method, this result may also be indicative of current challenges in obtaining reliable experimental carbon–proton SSCCs.

Williamson and coauthors measured experimental ^{13}C–^{1}H constants for another prominent organic molecule, cervinomycin A$_2$, (see Figure 4 for structure and numbering). Two sets of

Table 7. Experimental and Computed SSCCs (Hz) for Cervinomycin A$_2$

C	H	exp 1[a]	exp 2[b]	GIAO[c]	Δ_1	Δ_2	DU8c	Δ_1	Δ_2
C20	H16	5.4	4.7	5.2	0.2	−0.5	4.7	0.7	0.0
C18	H16	7.6	7.6	7.2	0.4	0.4	6.6	1.0	1.0
C15	H16	−5.9	−5.5	−4.2	−1.7	−1.3	−4.0	−1.9	−1.5
C17	H16		−3.4	−4.5		1.1	−4.3		0.9
C21	H16			1.9					
C27	H7	7.6	7.6	7.7	−0.1	−0.1	7.9	−0.3	−0.3
C25	H7	6.7	6.2	6.2	0.5	0	6.3	0.4	−0.1
C9	H7		5	5.9		−0.9	5.4		−0.4
C6	H7			1.1					
C8	H7	3.5		3.1	0.4		2.6	0.9	
C26	H7			−1.3					
C28	H7			1.1					
C23	H7			0.5					
C16	H19			1.1					
C20	H19			−1.7					
C18	H19		−2.2	−1.9		−0.3	−2.1		−0.1
C15	H19	10	9.4	10.2	−0.2	−0.8	9.9	0.1	−0.5
C17	H19	9	9	9.2	−0.2	−0.2	8.5	0.6	0.6
C21	H19	4.9	4.1	4.6	0.3	−0.5	4.7	0.2	−0.6
C7	H9	5.4	4.4	5.9	−0.5	−1.5	5.3	0.1	−0.9
C25	H9	5.8	6.6	6.2	−0.4	0.4	6.3	−0.5	0.3
C10	H9			2.1					
C11	H9	8.9	8.6	8.6	0.3	0	8.5	0.4	0.1
C24	H9			−1.5					
C8	H9		2	3.3		−1.3	2.7		−0.7
C13	H9			0.8					
C26	H9			0.9					
C23	H9			0.5					
C7	H10			0.1					
C25	H10			−1.1					
C24	H10	6	5.4	5.7	0.3	−0.3	5.8	0.2	−0.4
C8	H10	9	8.7	8.7	0.3	0	8.6	0.4	0.1
C13	H10			−0.3					
C12	H10	4.4	3.5	4	0.4	−0.5	4.2	0.2	−0.7
C23	H10			0.9					
number of exp SSCCs					15	18		15	18
rmsd (Hz)					0.6	0.7		0.7	0.6

[a]GB-CPMG-HSQMBC. [b]CLIP-HSQMBC. [c]DFT GIAO calculations (all in ref 14).

the SSCC data were reported from two different experiments, GB-CPMG-HSQMBC and CLIP-HSQMBC. Table 7 compares DU8c-computed carbon–proton spin–spin coupling constants with two experimental data sets and full spin–spin GIAO computations as carried out by the authors.

The example of cervinomycin A_2 provides additional evidence that DU8c (i) offers adequate accuracy in modeling experimental carbon–proton spin–spin coupling constants, (ii) performs on par with, if not better than, the state-of-the-art computational approaches utilizing explicit calculations of spin–orbit and other difficult contributions to Js, and (iii) offers dramatic reduction in computational times. Once again the inherent challenges of obtaining accurate carbon–proton nuclear spin–spin coupling constants are illustrated by the fact that the comparison of two experimental data sets in Table 7 yields an rmsd of 0.52 Hz. Although the proton–proton constants do not suffer to the same extent from this experimental limitation (i.e., DU8c-computed H–H constants of strychnine match the experimental values with an excellent rmsd of 0.17 Hz), it is not practical to expect accuracy better than 0.4–0.5 Hz from the C–H SSCC computations for the simple reason that the "bottleneck" in this case might be in the accuracy of the experimental measurements. As Parella et al.[21] observed: "The reason for... limited use of $^nJ_{CH}$ may be attributed to two main factors. First, there is no a single and general NMR method for their measurement... and, secondly, the accuracy of such measurements has always been a continuing source of discussion."

It appears that with the current version of the RFF the accuracy of computed carbon–proton constants became generally commensurate with the accuracy of the experimental state-of-the-art measurements. Granted, a similar level of accuracy is also approached by the high-end DFT computations (e.g., EPR-III basis set), which include explicit evaluation of spin dipolar, paramagnetic spin–orbit, and diamagnetic spin–orbit contributions. However, these latter calculations are exceedingly expensive. In contrast, the RFF approach is fast (by 2 orders of magnitude or better), and it also has a systematic mechanism for improvement. We are certain that with a larger training set, which is constantly being expanded as additional reliable experimental data becomes available, DU8c will produce increasingly accurate SSCCs in a mere fraction of the time required by the heavy spin–orbit computations.

CONCLUSIONS

The third generation Relativistic Force Field (RFF) parametrization method DU8c has been developed for scaling of Fermi contacts to compute accurate nuclear spin–spin coupling constants. The method utilizes a small empirical scaling set (24 parameters for C–H and 17 for H–H SSCCs) in conjunction with hybridization correction based on NBO coefficients. The method achieves 0.4–0.8 Hz accuracy in predicting carbon–proton SSCCs (2.3 Hz for ^1J), which is adequate for guiding and informing the process of structure determination. Most importantly, this accuracy is achieved with drastically reduced computational times, which should allow for fast and accurate predictions of NMR spectra in conformationally flexible organic molecules, where averaging is necessarily performed over an ensemble of conformers. These developments will be all the more important, as more NMR experiments, such as J-resolved HMBC,[22] HETLOC,[23] or selective HSQMBC-TOCSY-IPAP,[19] etc., producing accurate

^{13}C–^1H SSCCs for stereochemical assignment become mainstream in the organic toolbox.

ASSOCIATED CONTENT

Ⓢ Supporting Information

The Supporting Information is available free of charge on the ACS Publications website at DOI: 10.1021/acs.joc.5b02001.

Computational details, structures, and computed SSCCs (PDF)

AUTHOR INFORMATION

Corresponding Author

*E-mail: akutatel@du.edu.

Notes

The authors declare no competing financial interest.

ACKNOWLEDGMENTS

REFERENCES

(1) (a) Onak, T.; Jaballas, J.; Barfield, M. *J. Am. Chem. Soc.* **1999**, *121*, 2850. (b) Scheurer, C.; Bruschweiler, R. *J. Am. Chem. Soc.* **1999**, *121*, 8661. (c) Del Bene, J. E.; Bartlett, R. J. *J. Am. Chem. Soc.* **2000**, *122*, 10480. (d) Del Bene, J. E.; Perera, S. A.; Bartlett, R. J. *J. Am. Chem. Soc.* **2000**, *122*, 3560. (e) Del Bene, J. E.; Perera, S. A.; Bartlett, R. J. *J. Phys. Chem. A* **2001**, *105*, 930. (f) Diez, E.; Casanueva, J.; San Fabian, J.; Esteban, A. L.; Galache, M. P.; Barone, V.; Peralta, J. E.; Contreras, R. H. *Mol. Phys.* **2005**, *103*, 1307.

(2) Bally, T.; Rablen, P. R. *J. Org. Chem.* **2011**, *76*, 4818.

(3) Kutateladze, A. G.; Mukhina, O. A. *J. Org. Chem.* **2014**, *79*, 8397.

(4) Wilkens, S. J.; Westler, W. M.; Markley, J. L.; Weinhold, F. *J. Am. Chem. Soc.* **2001**, *123*, 12026.

(5) (a) Foster, J. P.; Weinhold, F. *J. Am. Chem. Soc.* **1980**, *102*, 7211. (b) Reed, A. E.; Weinhold, F. *J. Chem. Phys.* **1983**, *78*, 4066. (c) Reed, A. E.; Weinstock, R. B.; Weinhold, F. *J. Chem. Phys.* **1985**, *83*, 735.

(6) Kutateladze, A. G.; Mukhina, O. A. *J. Org. Chem.* **2015**, *80*, 5218.

(7) For reviews and recent overviews of the theory of spin–spin coupling constants in NMR spectra and utilization of computations for predicting spectra of complex organic compounds, see: (a) San Fabian, J.; Garcia de la Vega, J. M.; San Fabian, E. *J. Chem. Theory Comput.* **2014**, *10*, 4938. (b) Helgaker, T.; Coriani, S.; Jorgensen, P.; Kristensen, K.; Olsen, J.; Ruud, K. *Chem. Rev.* **2012**, *112*, 543. (c) Rusakov, Yu. Yu.; Krivdin, L. B. *Russ. Chem. Rev.* **2013**, *82*, 99. (d) Bifulco, G.; Dambruoso, P.; Gomez-Paloma, L.; Riccio, R. *Chem. Rev.* **2007**, *107*, 3744. (e) Jensen, F. *J. Chem. Theory Comput.* **2006**, *2*, 1360. (f) Maximoff, S. N.; Peralta, J. E.; Barone, V.; Scuseria, G. E. *J. Chem. Theory Comput.* **2005**, *1*, 541.

(8) dos Santos, F. P.; Tormena, C.; Contreras, R. H.; Rittner, R.; Magalhães. *Magn. Reson. Chem.* **2008**, *46*, 107.

(9) Woon, D. E.; Dunning, T. H. *J. Chem. Phys.* **1993**, *98*, 1358.

(10) Barone, V. *J. Chem. Phys.* **1994**, *10*, 6834.

(11) (a) Zimmerman, H. E.; Kutateladze, A. G. *J. Am. Chem. Soc.* **1996**, *118*, 249. (b) Zimmerman, H. E.; Kutateladze, A. G. *J. Org. Chem.* **1995**, *60*, 6008.

(12) (a) Pretsch, E.; Bühlmann, P.; Badertscher, M. *Structure Determination of Organic Compounds. Tables of Spectral Data*. 4th Ed.; Sringer, 2009. (b) Neto, A. C.; dos Santos, F. P.; Contreras, R. H.; Rittner, R.; Tormena, C. F. *J. Phys. Chem. A* **2008**, *112*, 11956. (c) Parella, T.; Sanchez-Ferrando, F.; Virgili, A. *Magn. Reson. Chem.* **1997**, *35*, 30. (d) Parella, T.; Sanchez-Ferrando, F.; Virgili, A. *Magn. Reson. Chem.* **1995**, *33*, 196. (e) Parella, T.; Sanchez-Ferrando, F.; Virgili, A. *Magn. Reson. Chem.* **1994**, *32*, 657. (f) Parella, T.; Casas, R.; Ortuno, R. M. *Magn. Reson. Chem.* **1992**, *30*, 1084. (g) Denisov, A.Yu.; Tyshchishin, E. A.; Tkachev, A. V.; Mamtyuk, V. I. *Magn. Reson. Chem.*

1992, *30*, 886. (h) Hansen, P. E. *Prog. Nucl. Magn. Reson. Spectrosc.* **1981**, *14*, 175.

(13) Latest version of the NBO program, NBO 6.0: Glendening, E. D.; Badenhoop, K.; Reed, A. E.; Carpenter, J. E.; Bohmann, J. A.; Morales, C. M.; Landis, C. R.; Weinhold, F. *Theoretical Chemistry Institute*; University of Wisconsin: Madison, 2013.

(14) Williamson, R. T.; Buevich, A. V.; Martin, G. E.; Parella, T. *J. Org. Chem.* **2014**, *79*, 3887.

(15) Method MI (a), method MII (b), and method MIII (c), as described in: Edden, R. A. E.; Keeler, J. *J. Magn. Reson.* **2004**, *166*, 53.

(16) Blechta, V.; del Rio-Portilla, F.; Freeman, R. *Magn. Reson. Chem.* **1994**, *32*, 134.

(17) Marquez, B. L.; Gerwick, W. H.; Williamson, R. T. *Magn. Reson. Chem.* **2001**, *39*, 499.

(18) Misiak, M.; Kozminski, W. *Magn. Reson. Chem.* **2009**, *47*, 205.

(19) Sauri, J.; Espinosa, J. F.; Parella, T. *Angew. Chem., Int. Ed.* **2012**, *51*, 3919.

(20) IPAP-HSQMBC (a) and IPAP-HSQC-TOCSY (b), as described in: Gil, S.; Espinosa, J. F.; Parella, T. *J. Magn. Reson.* **2010**, *207*, 312.

(21) Gil, S.; Espinosa, J. F.; Parella, T. *J. Magn. Reson.* **2011**, *213*, 145.

(22) Meissner, A.; Sørensen, O. W. *Magn. Reson. Chem.* **2001**, *39*, 49.

(23) Kurz, M.; Schmieder, P.; Kessler, H. *Angew. Chem., Int. Ed. Engl.* **1991**, *30*, 1329.